ELSEVIER

Thermochimica Acta 253 (1995) 19–31

thermochimica acta

Heat capacity measurement on $(Zr_{1-y}M_y)O_x$ (where M is Nb, Sn) from 325 to 905 K ☆

Toshihide Tsuji *, Masaki Amaya, Keiji Naito

Department of Nuclear Engineering, Faculty of Engineering, Nagoya University, Furo-cho, Chikusa-ku, Nagoya 464-01, Japan

Received 23 June 1994; accepted 7 July 1994

Abstract

Heat capacities of $(Zr_{1-y}M_y)O_{0.17}$ and $(Zr_{1-y}M_y)O_{0.28}$ (where M is Nb or Sn, $y = 0$–0.07) having α''-$ZrO_{\approx 1/6}$-type and α''-ZrO_x-type crystal structures, respectively, were measured from 325 to 905 K using an adiabatic scanning calorimeter. A heat capacity anomaly at higher temperatures due to an order–disorder rearrangement of interstitial oxygen atoms in zirconium based alloys was observed for all samples, after the heat capacity anomaly at lower temperatures had been attributed to a non-equilibrium phenomenon. The transition temperature, transition enthalpy and entropy changes due to the order–disorder transition decreased with increasing doped niobium or tin content, indicating that arrangement of oxygen atoms in the lower temperature phase may be partially disordered by substituting niobium or tin for zirconium. The entropy change due to the order–disorder transition for $(Zr_{1-y}M_y)O_{0.17}$ and $(Zr_{1-y}M_y)O_{0.28}$ solid solutions was compared with the theoretical value. The solubility limits of $(Zr_{1-y}M_y)O_{0.17}$ and $(Zr_{1-y}M_y)O_{0.28}$ were determined from the variation of lattice constants, transition temperature, transition enthalpy and entropy changes against niobium or tin content.

Keywords: Heat capacity; Order–disorder transition; Zr–O alloy; $(Zr_{1-y}Nb_y)O_x$; $(Zr_{1-y}Sn_y)O_x$

* Corresponding author.

☆ Presented at the International and III Sino–Japanese Symposium on Thermal Measurements, Xi'an, 4–6 June 1994.

SSDI 0040-6031(94)02023-X

1. Introduction

The α-zirconium phase dissolves oxygen atoms up to 30 at.% in the octahedral interstices of the h.c.p. zirconium lattice at room temperature, forming ordered structures at higher oxygen compositions and lower temperatures. Hirabayashi and co-workers [1–5] have reported that there are three order and disorder phases in zirconium–oxygen alloys; the completely ordered phase α″, the intra layer disordered phase α′ and the completely disordered phase α. The λ-type heat capacity anomaly due to an order–disorder transition is expected to be observed from heat capacity measurement of ZrO_x with constant composition.

Arai and Hirabayashi [6] measured the heat capacities of the ZrO_x ($x = 0.16$–0.41) alloys and obtained enthalpy and entropy changes for the order–disorder transition for zirconium–oxygen alloys, but did not calculate the theoretical transition entropy change. We also measured heat capacities of zirconium–oxygen alloys ZrO_x ($x = 0.17$, 0.20, 0.28 and 0.31) from 325 to 905 K using an adiabatic scanning calorimeter [7]. Two types of heat capacity anomaly were observed in all the samples: one was the anomaly at lower temperatures due to a non-equilibrium phenomenon which was not observed by Arai and Hirabayashi [6] and the other was the λ-type anomaly at higher temperatures assigned to an order–disorder rearrangement of oxygen atoms. The entropy change due to the order–disorder transition for Zr–O solid solution measured in our previous work was larger than that measured by Arai and Hirabayashi [6], but was in fairly good agreement with the theoretical value. The heat capacities of niobium or tin doped ZrO_x alloys were also measured in our previous work [7,8]. The transition temperature, transition enthalpy and entropy changes due to the order–disorder transition decreased with increasing niobium or tin content, and the doping effect was qualitatively discussed in terms of the interaction between doped metal and oxygen atoms.

In this paper, heat capacities of $(Zr_{1-y}M_y)O_{0.17}$ and $(Zr_{1-y}M_y)O_{0.28}$ (where M is Nb or Sn, $y = 0$–0.07) having α″-$ZrO_{\approx 1/6}$-type and α″-ZrO_x-type crystal structures, respectively, were measured from 325 to 905 K in order to determine quantitatively the effect of doped niobium and tin contents on the transition mechanism from the transition temperatures, transition enthalpy and entropy changes for the order–disorder transitions, compared with the theoretical entropy changes.

2. Experimental

2.1. Sample preparation

Doped samples of $(Zr_{1-y}M_y)O_{0.17}$ and $(Zr_{1-y}M_y)O_{0.28}$ (where M is Nb or Sn, $y = 0$–0.07) were prepared using a method similar to that used to prepare zirconium–oxygen alloys in an earlier study [7]. Zirconium metal sponge of 99.6% purity containing the impurities hafnium, iron, oxygen, nitrogen, etc., zirconium metal oxidized at 773 K in air and metal powders (niobium or tin) of 99.99% purity were mixed in an appropriate ratio and melted a few times using a plasma jet furnace

under an argon gas stream. The cast sample obtained was sealed in a quartz tube, annealed for 3 days at 1273 K, and cooled to room temperature over a period of 3 days. The sample was crushed into pieces of less than 3 mm size using a stainless-steel mortar. About 20 g of the crushed sample was sealed in a quartz vessel filled with helium gas at 20 kPa, and annealed at 873 K for 2 weeks, then at 500 K for 2 weeks and cooled slowly to room temperature over a period of 3 days to obtain a highly ordered phase, and this sample was used for heat capacity measurement. The identification of phase and the measurement of lattice constants of the samples were carried out by X-ray diffractometry. The chemical compositions of the sample were measured by an electron probe microanalyzer. The O/(Zr + M) (where M is Nb or Sn) ratio of the sample was determined from the mass gain by oxidizing it to ZrO_2 and Nb_2O_5 or SnO_2 at 1273 K in air for 1 week.

2.2. Heat capacity measurement

Heat capacities of $(Zr_{1-y}M_y)O_{0.17}$ and $(Zr_{1-y}M_y)O_{0.28}$ (where M is Nb or Sn, $y = 0-0.07$) were measured using an adiabatic scanning calorimeter [9]; in this calorimeter the power supplied to the sample was measured continuously, and the heating rate was kept constant regardless of the type and amount of the sample. The heating rate chosen was 2 K min^{-1}, and the measurement was carried out between 325 and 905 K under a pressure of about 130 Pa of air using a sample of about 20 g sealed in a quartz vessel filled with helium gas at 20 kPa. The heating rate and adiabatic control were usually maintained within ± 0.005 K min^{-1} and ± 0.01 K, respectively. The heat capacity measurement was conducted within an imprecision of $\pm 2\%$ and an inaccuracy of $\pm 2\%$.

3. Results and discussion

3.1. Lattice constants of $(Zr_{1-y}M_y)O_{0.17}$ and $(Zr_{1-y}M_y)O_{0.28}$ (where M is Nb or Sn)

Figs. 1(a) and (b) show the variation of the lattice constants of a and c axes, respectively, as a function of y for $(Zr_{1-y}M_y)O_{0.17}$ and $(Zr_{1-y}M_y)O_{0.28}$ (where M is Nb or Sn, $y = 0-0.07$). In Fig. 1 the lattice constants of undoped α''-ZrO_x measured by Yamaguchi [1] and Holmberg and Dagerhamn [10] are also shown for comparison. As seen in the figure, our data are in good agreement with their data. In Figs. 1(a) and (b), the break points are seen in the plots of the lattice constants of a and c axes for $(Zr_{1-y}M_y)O_{0.17}$ and $(Zr_{1-y}M_y)O_{0.28}$ samples against niobium or tin doped contents. The intermetallic compound Zr_5Sn_3 was observed only in samples having y values higher than those at $y = 0.045$ for $(Zr_{1-y}Sn_y)O_{0.17}$ and at $y = 0.015$ for $(Zr_{1-y}Sn_y)O_{0.28}$, and these break points are regarded as the solubility limits of tin at constant O/M ratio. However, for niobium doped compounds no intermetallic compounds except main peaks were observed, probably because of the small content of doped niobium. The break points at $y = 0.005$ for $(Zr_{1-y}Nb_y)O_{0.17}$

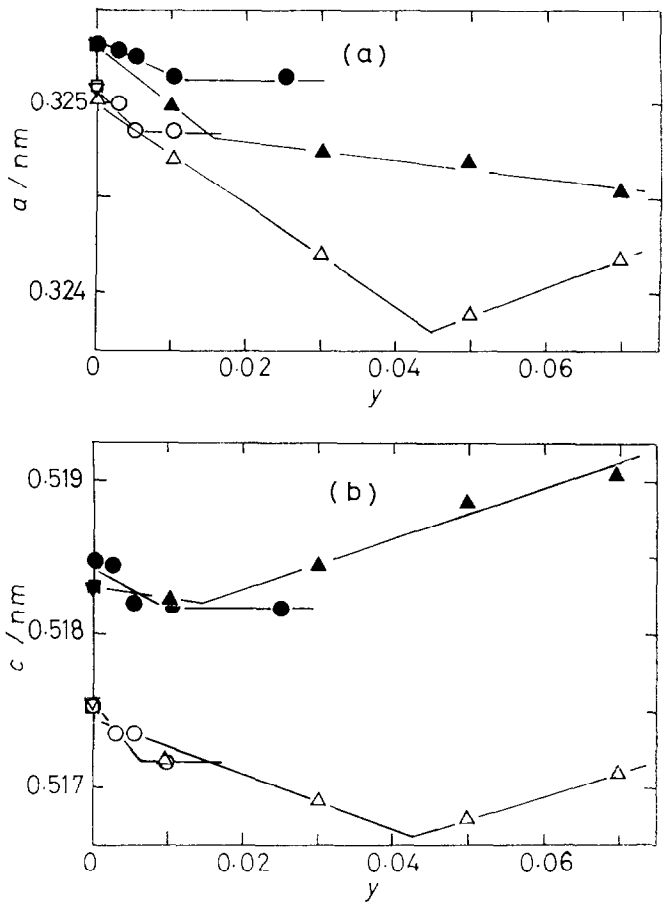

Fig. 1. Variation of the lattice constants of (a) a and (b) c axes as a function of y for $(Zr_{1-y}M_y)O_{0.17}$ (○, △, □, ▽) and $(Zr_{1-y}M_y)O_{0.28}$ (●, ▲, ■, ▼) (where M is Nb or Sn, $y = 0$–0.07); ○, ●, M is Nb in this work; △, ▲, M is Sn in this work; □, ■, $y = 0$ by Yamaguchi [1]; ▽, ▼, $y = 0$ by Holmberg and Dagerhamn [10].

and $y = 0.01$ for $(Zr_{1-y}Nb_y)O_{0.28}$ seen in Figs. 1(a) and (b) are considered to be the solubility limit of niobium at constant O/M ratio.

3.2. Heat capacity of $(Zr_{1-y}M_y)O_{0.17}$ (where M is Nb or Sn)

The results of the heat capacity measurements on $(Zr_{1-y}Sn_y)O_{0.17}$ ($y = 0$, 0.01 and 0.03) are shown in Figs. 2(a), (b) and (c), respectively. The solid lines in the figures are baselines of heat capacity. The baseline of the heat capacity for undoped ZrO_x was determined from analysis of heat capacity by the same procedures as described in our previous paper [7], and the baseline for the doped $(Zr_{1-y}Sn_y)O_x$

sample is assumed to be the same as that for the undoped sample, because of small dopant contents.

Two types of heat capacity anomalies are seen in Figs. 2(a), (b) and (c) for $(Zr_{1-y}Sn_y)O_{0.17}$ ($y = 0$, 0.01 and 0.03, respectively): the broad peak at about 500 K (we designate it the low temperature heat capacity anomaly in this paper) and the sharp peak seen in the temperature range 600–700 K (we designate it the high temperature heat capacity anomaly).

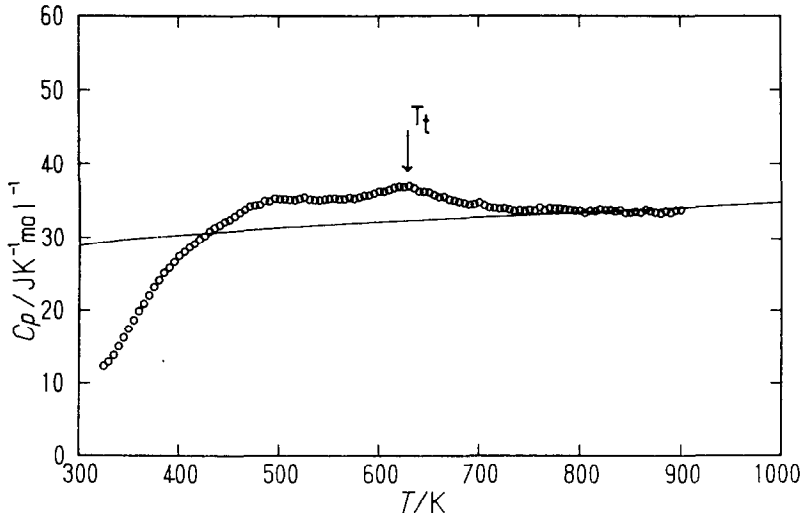

(a)

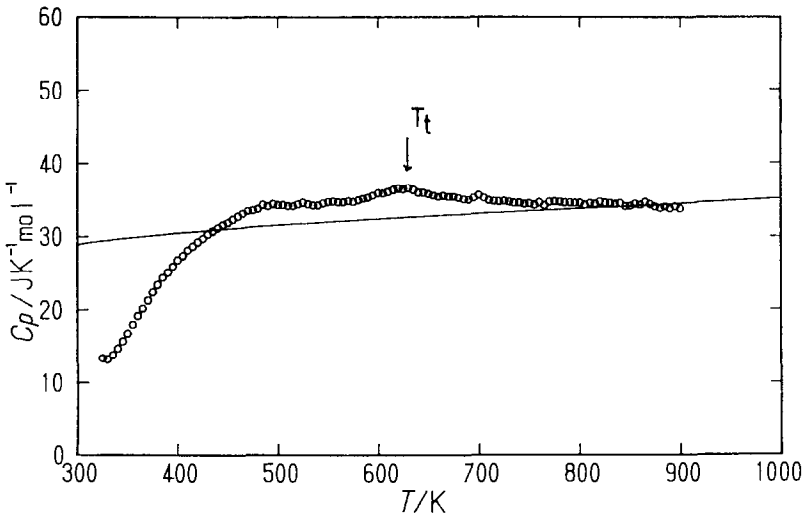

(b)

Fig. 2(a) and (b)

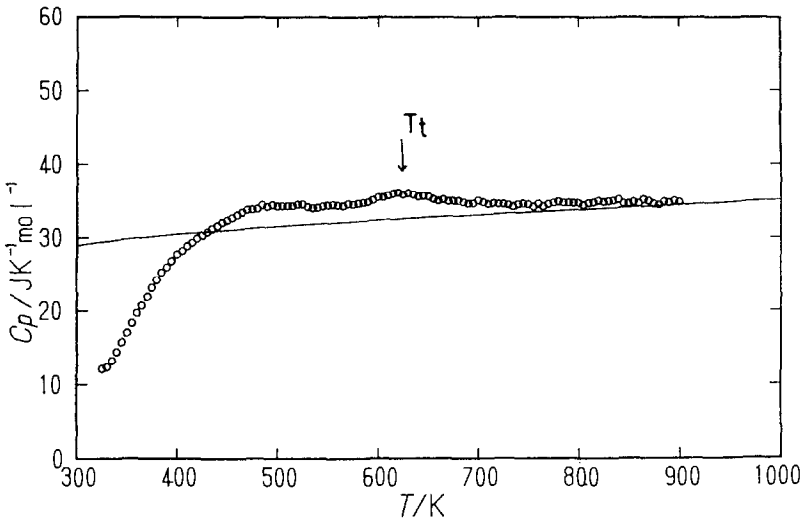

(c)

Fig. 2. Heat capacities of $(Zr_{1-y}Sn_y)O_{0.17}$: (a) $y = 0$; (b) $y = 0.01$; (c) $y = 0.03$. The transition temperature T_t corresponds to the phase transition from the completely ordered phase α'' to the completely disordered phase α.

The low temperature heat capacity anomaly at about 500 K seen in Fig. 2 has been observed in our laboratory for V–O [11,12], Ti–O [13] and Zr–O solid solutions [7]. These anomalies are considered as exo- and endothermic reactions by the relaxation of thermal non-equilibrium states as explained qualitatively elsewhere [7,12].

The high temperature heat capacity anomaly observed for undoped and doped $(Zr_{1-y}Sn_y)O_{0.17}$ in the temperature range 600–700 K seen in Fig. 2 is thought to be due to the order–disorder rearrangement of the interstitial oxygen atoms in zirconium based host lattices: the transition temperature T_t corresponds to phase transition from the completely ordered phase α'' to the completely disorderd phase α as discussed in our previous paper [7]. The transition temperature T_t is defined as the temperature at which the heat capacity value shows a peak. The error of the transition temperature is estimated to be ± 6 K from heat capacity data measured by changing the heating rate from 1 to 4 K min^{-1}. The transition temperature of undoped sample obtained in this study was in good agreement with that obtained by Arai and Hirabayashi [6].

The excess heat capacities of $(Zr_{1-y}M_y)O_{0.17}$ (where M is Nb or Sn, $y = 0$–0.07) due to the order–disorder transitions are estimated in a manner similar to that adopted in our previous study [7] and the results for transition enthalpy (ΔH) and entropy (ΔS) changes are shown in Figs. 3(b) and (c), respectively, together with the transition temperature T_t in Fig. 3(a) as a function of niobium or tin content. The errors of transition enthalpy and entropy changes are estimated from the experimental data to be ± 0.05 kJ mol^{-1} and ± 0.06 J K^{-1} mol^{-1}. It is also seen

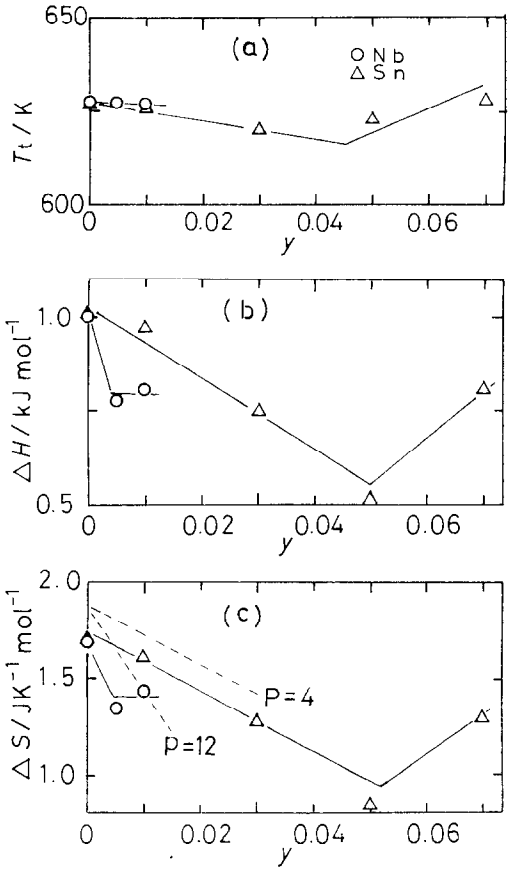

Fig. 3. (a) Transition temperature T_t, (b) transition enthalpy ΔH and (c) entropy ΔS changes as a function of doped niobium or tin content. In (c), the dashed lines are the theoretical entropy changes due to the order–disorder transition of oxygen atoms from the partially ordered phase (α''-$ZrO_{\approx 1/6}$-type crystal structure shown in Fig. 4(a)) to the completely disordered phase α ($p = 12$ for niobium and $p = 4$ for tin).

from Figs. 3(a)–(c) that the solubility limits of niobium and tin in the $(Zr_{1-y}M_y)O_{0.17}$ samples are around $y = 0.005$ and $y = 0.045$, respectively, as expected from the plots of lattice constants against niobium or tin contents in Fig. 1. As can be seen in Fig. 3, the transition temperatures, transition enthalpy and entropy changes decrease slightly with increasing niobium or tin content within the solubility limit. The decrease in the transition enthalpy and entropy changes with increasing doped metal content may be explained in the following way. Because the substitution of doped atoms for zirconium sites causes partial disordering of oxygen atoms in the low temperature phase, the difference in regularity between ordered and disordered states in a doped sample is smaller than that in an undoped sample.

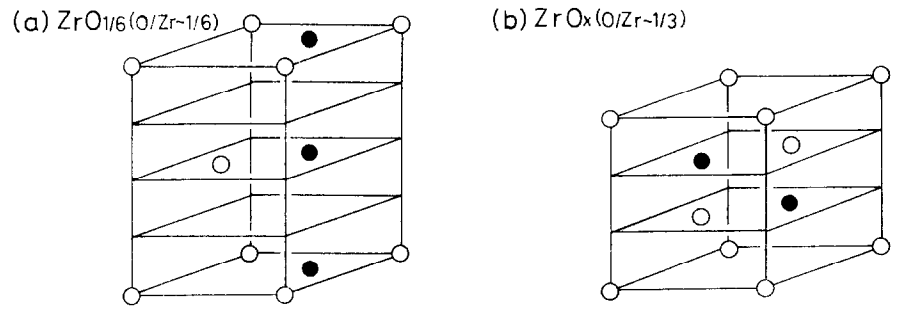

Fig. 4. Typical ordered structures of (a) α''-$ZrO_{\approx 1/6}$ and (b) α''-ZrO_x ($x < 1/3$) proposed by Arai and Hirabayashi [6], where only oxygen atom sites are depicted as open circles. In the figure the filled circles show additional oxygen atom sites considered by the present authors. These partially ordered structures where oxygen atoms occupy both open and filled circles are used for calculation of the theoretical transition entropy change.

The ordered crystal structures of α''-$ZrO_{\approx 1/6}$ and α''-ZrO_x ($x < 1/3$) corresponding to the composition α''-$ZrO_{0.17}$ and α''-$ZrO_{0.28}$, respectively, were determined by X-ray, electron and neutron diffraction methods by Arai and Hirabayashi [6] and their crystal structures are shown in Figs. 4(a) and (b), respectively, where only oxygen atom sites are depicted as open circles. The theoretical entropy change for undoped sample calculated on the basis of the crystal structure (open circles) shown in Fig. 4(a) was larger than the experimental value. Thus additional oxygen atom sites shown as filled circles in the figure were considered in our previous paper [8]. This partially ordered structure where oxygen atoms occupy both open and filled circles is used for calculation of the theoretical transition entropy change of undoped and doped samples as will be shown below. In Fig. 3(c), the dotted lines are the theoretical entropy changes due to the order–disorder transition of oxygen atoms from the partially ordered phase (α''-$ZrO_{\approx 1/6}$-type crystal structure shown in Fig. 4(a)) to the completely disordered phase α. The theoretical entropy change is calculated on the basis of the following three assumptions. (1) Because the ionic radius of niobium or tin is smaller than that of zirconium, the lattice constants of a and c axes of $(Zr_{1-y}M_y)O_x$ (where M is Nb or Sn) decrease with the increase of substitutional niobium or tin doped content as seen in Fig. 1, thereby causing neighboring zirconium atoms near niobium or tin atoms to come closer and preventing oxygen atoms from occupying normal positions in the ordered structure as shown in Fig. 4(a). Therefore, every substitution of a doped atom for a zirconium atom blocks the "p" sites of normal oxygen positions. (2) The numbers of oxygen atoms blocked by every niobium or tin atom are "p" atoms, irrespective of whether it is an ordered or a disordered structure. (3) The ordered structure of $(Zr_{1-y}M_y)O_{0.17}$ is derived from that of undoped α''-$ZrO_{\approx 1/6}$ as shown in Fig. 4(a). The theoretical entropy change, dS_1, is calculated from the following equation by using Stirling's approximation

$$
\begin{aligned}
\mathrm{d}S_1 &= k\ \ln\{_{(1-yp)N}C_{Nx}\} - k\ \ln[_{\{4N/12(1-yp)\}}C_{Nx}] \\
&\approx R\{(1-yp)\ \ln(1-yp) - (1-yp-x)\ \ln(1-yp-x) \\
&\quad +[1/\{3(1-yp)\}]\ \ln\{3(1-yp)\} \\
&\quad +[1/\{3(1-yp)\}-x]\ \ln[1/\{3(1-yp)\}-x]\}
\end{aligned} \tag{1}
$$

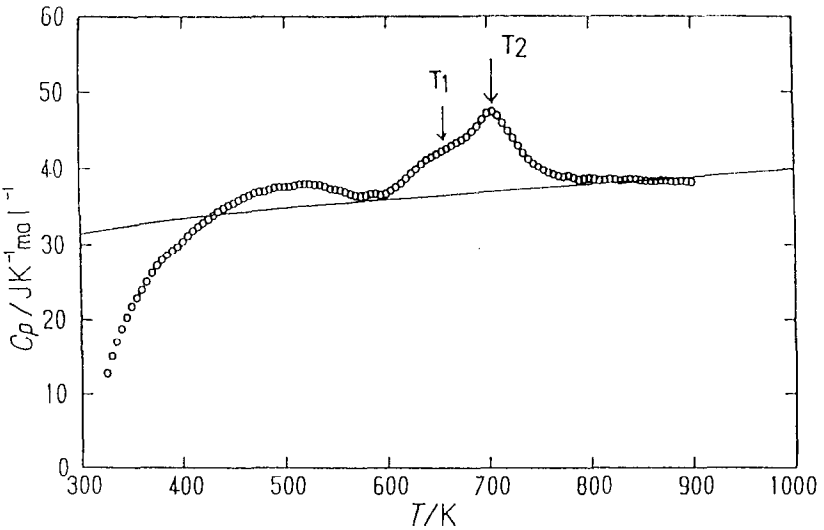

(a)

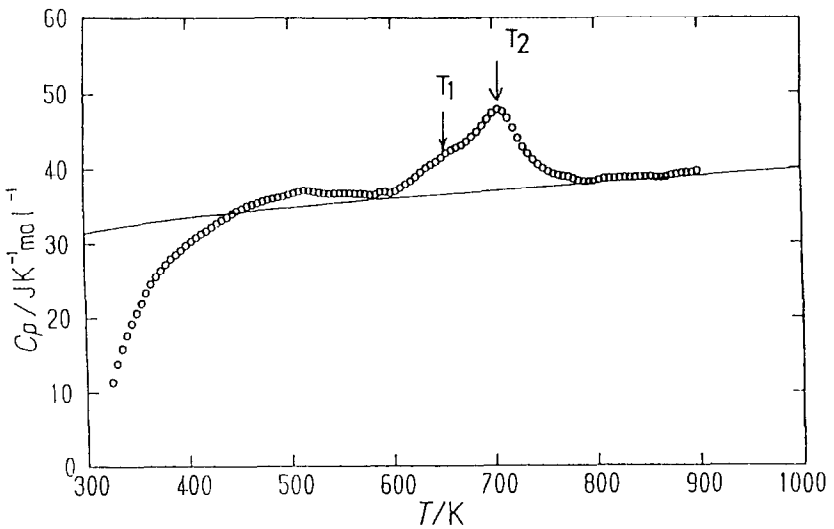

(b)

Fig. 5 (a) and (b)

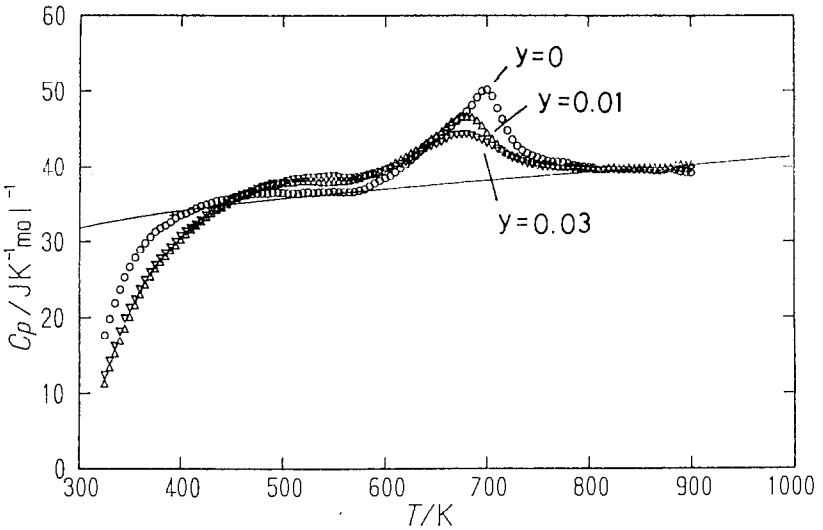

Fig. 5. Heat capacities of $(Zr_{1-y}M_y)O_{0.28}$: (a) $ZrO_{0.28}$, (b) $(Zr_{0.995}Nb_{0.005})O_{0.28}$ and (c) $(Zr_{1-y}Sn_y)O_{0.28}$ ($y = 0$, 0.01 and 0.03). The transition temperatures T_1 and T_2 correspond to phase transition from the completely ordered phase α'' to two phases of α-ZrO_x + LPSS (long period stacking structure) and that from α-ZrO_x + LPSS to the completely disordered phase α, respectively [6].

where k is Boltzmann's constant and N is Avogadro's number. As seen in Fig. 3(c), the slopes of the plots of the experimental transition entropies of doped samples as a function of y obtained in this study are in good agreement with those of the theoretical values of dS_1 calculated by putting $p = 12$ and $p = 4$ for niobium and tin doped samples in Eq. (1), respectively.

3.3. Heat capacity of $(Zr_{1-y}M_y)O_{0.28}$ (where M is Nb or Sn)

The results of heat capacity measurements of $ZrO_{0.28}$, $(Zr_{0.995}Nb_{0.005})O_{0.28}$ and $(Zr_{1-y}Sn_y)O_{0.28}$ ($y = 0$, 0.01 and 0.03) samples in the temperature range 325–905 K are shown in Figs. 5(a), (b) and (c), respectively. In Fig. 5(c) heat capacities of tin doped samples are in good agreement with that of the undoped $ZrO_{0.28}$ sample in the temperature range 800–900 K. The solid line in the figure is a baseline of heat capacity which is determined by the same procedures as described in our previous paper [7]. The low temperature heat capacity anomalies at about 500 K as seen in Fig. 5 are considered as exo- and endothermic reactions by the relaxation of thermal non-equilibrium states as discussed for $(Zr_{1-y}M_y)O_{0.17}$ samples. Two high temperature heat capacity anomalies (T_1 and T_2) were observed for undoped $ZrO_{0.28}$ and niobium doped $(Zr_{0.995}Nb_{0.005})O_{0.28}$ samples in the temperature range 650–720 K as seen in Figs. 5(a) and (b), respectively; the transition temperatures T_1 and T_2 correspond to phase transition from the completely ordered phase α'' to two phases of α-ZrO_x + LPSS (long period stacking structure) and that from α-

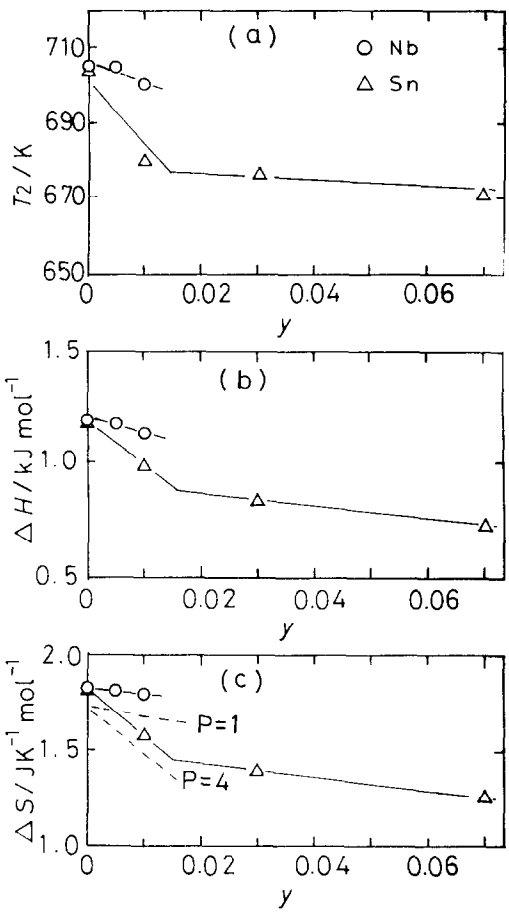

Fig. 6. (a) Transition temperature T_1, (b) transition enthalpy ΔH and (c) entropy ΔS changes as a function of doped niobium or tin content. In (c) the dashed lines are the theoretical entropy changes due to the order–disorder transition of oxygen atoms from the partially ordered phase (α''-ZrO_x-type crystal structure shown in Fig. 4(b)) to the completely disordered phase α ($p = 1$ for niobium and $p = 4$ for tin).

ZrO_x + LPSS to the completely disordered phase α, respectively [6]. The average transition temperature of T_1 and T_2 for undoped sample in this study is in good agreement with that found by Arai and Hirabayashi [6], although their experiments could not resolve two peaks. The transition temperature T_1 is not observed for tin doped samples as seen in Fig. 5(c). The transition temperature T_2, transition enthalpy ΔH and entropy ΔS changes of doped samples together with undoped sample obtained in this study are shown in Figs. 6(a), (b) and (c), respectively, as a function of doped niobium or tin content. As can be seen in Fig. 6, the transition temperatures, transition enthalpy and entropy changes decrease slightly with increasing doped niobium or tin content within the solubility limit, indicating that the

substitution of niobium or tin atoms for zirconium sites causes partial disordering of oxygen atoms at the low temperature phase, and the difference in regularity between ordered and disordered states of doped sample is smaller than that of undoped sample.

In Fig. 6(c), the dotted lines are the theoretical entropy changes due to the order–disorder transition of oxygen atoms from the partially ordered phase (α''-ZrO_x-type crystal structure shown in Fig. 4(b)) to the completely disordered phase α, and the theoretical entropy change dS_2 is calculated from the following equation by using Stirling's approximation

$$\begin{aligned} dS_2 &= k\ \ln\{{}_{(1-yp)N}C_{Nx}\} - k\ \ln[{}_{5N/\{9(1-yp)\}}C_{Nx}] \\ &\approx R\{(1-yp)\ \ln(1-yp) - (1-yp-x)\ \ln(1-yp-x) \\ &\quad -[5/\{9(1-yp)\}]\ \ln[5/\{9(1-yp)\}] \\ &\quad +[5/\{9(1-yp)\}-x]\ \ln[5/\{9(1-yp)\}-x]\} \end{aligned} \tag{2}$$

The slopes of the plots of the experimental transition entropies of doped samples as a function of y obtained in this study are in good agreement with those of the theoretical values of dS_2 calculated by putting $p = 1$ and $p = 4$ for niobium and tin doped samples in Eq. (2), respectively. The values of p for tin doped samples are the same ($p = 4$) for $(Zr_{1-y}Sn_y)O_{0.17}$ and $(Zr_{1-y}Sn_y)O_{0.28}$ samples, but those for niobium doped samples are different ($p = 12$ for $(Zr_{1-y}Nb_y)O_{0.17}$ and $p = 1$ for $(Zr_{1-y}Nb_y)O_{0.28}$). This difference may be related to the fact that tin and oxygen stabilize the α phase of zirconium, whereas niobium stabilizes the β phase. It is also seen in Figs. 6(a)–(c) that the solubility limit of $(Zr_{1-y}M_y)O_{0.28}$ sample is around the composition $y = 0.015$ for tin doped sample as expected from the plots of lattice constants against tin content in Fig. 1.

Acknowledgment

The authors are indebted to Mr. K. Abe of Kobe Steel, Ltd., Hyogo, Japan for sample preparation and chemical analysis of the samples.

References

[1] S. Yamaguchi, J. Phys. Soc. Jpn., 24 (1968) 855.
[2] S. Yamaguchi and M. Hirabayashi, J. Appl. Crystallogr., 3 (1970) 319.
[3] S. Hashimoto, H. Iwasaki, S. Ogawa, S. Yamaguchi and M. Hirabayashi, J. Appl. Crystallogr., 7 (1974) 67.
[4] M. Hirabayashi, S. Yamaguchi, T. Arai, H. Asano and S. Hashimoto, Phys. Status Solidi A, 23 (1974) 331.
[5] S. Hashimoto, J. Appl. Crystallogr., 8 (1975) 243.
[6] T. Arai and M. Hirabayashi, J. Less-Common Met., 44 (1976) 291.
[7] T. Tsuji, M. Amaya and K. Naito, J. Therm. Anal., 38 (1992) 1817.
[8] T. Tsuji, M. Amaya and K. Naito, J. Nucl. Mater., 201 (1993) 126.

[9] K. Naito, H. Inaba, M. Ishida, Y. Saito and H. Arima, J. Phys. E, 7 (1974) 464.
[10] B. Holmberg and T. Dagerhamn, Acta Chem. Scand., 15 (1961) 919.
[11] K. Naito, H. Inaba and S. Tsujimura, unpublished work.
[12] T. Matsui, T. Tsuji, T. Asano and K. Naito, Thermochim. Acta, 183 (1991) 1.
[13] T. Tsuji, M. Sato and K. Naito, Thermochim. Acta, 163 (1990) 279.